Supporting Information

Three-dimensional perchlorate-based alkali metal hybrid perovskite molecular ferroelastic crystals

Yu-Si Liu,[a] Zhe-Kun Xu,[a] Jia-Mei Zhang,[a] Xiao-Gang Chen,[a] Yan Qin,[a] and Zhong-Xia Wang*[ab]

[a]*Ordered Matter Science Research Center, Nanchang University, Nanchang 330031, People's Republic of China*
[b]*College of Chemistry and Chemical Engineering, Gannan Normal University, Ganzhou 341000, People's Republic of China*
E-mail address: zhongxiawang@ncu.edu.cn

Experimental Section

Materials. The reagents 1,4-diazabicyclo[2.2.2]octane (DABCO), K_2CO_3, Rb_2CO_3, Cs_2CO_3, perchloric acid (70%~72%), iodomethane and bromofluoromethane were purchased from companies and used as received. The solvent-deionized water, tetrahydrofuran and ethyl ether were purchased from Aladdin and used without further purification.

Synthesis of MDABCO iodized salt. The synthesis method is according to the former reports.[1] At room temperature, CH_3I (14.9 g, 105 mmol) was added dropwise to the solution of 1,4-diazabicyclo[2.2.2]octane (11.21 g, 100 mmol) dissolved in tetrahydrofuran (300 ml) and kept stirring for more than 5 hrs. As the drip went on, a large number of white precipitates were generated gradually. Then the precipitates were filtered and washed with ether more than three times. The white solid was dried under reduced pressure and collected as the product (23.4 g, 92 %). ^{1}H NMR (300 MHz, Deuterium Oxide) δ 3.34 (t, J = 7.5 Hz, 6H), 3.13 (t, J = 7.6 Hz, 6H), 3.00 (s, 3H). ^{13}C NMR (75 MHz, Deuterium Oxide) δ 54.06, 54.02, 53.97, 51.69, 51.63, 51.57, 44.24. ESI MS m/z. Calc. for $[M]^+$ 127.1; Found 127.1.

Synthesis of FMDABCO bromide salt. The synthesis method is the same as that of the former, except that iodomethane is replaced by fluorobromomethane and the yield is 89 %. ^{1}H NMR (300 MHz, Deuterium Oxide) δ 5.28 (d, J = 45.0 Hz, 2H), 3.54 – 3.39 (m, 6H), 3.30 – 3.11 (m, 6H).^{19}F NMR (282 MHz, Deuterium Oxide) δ -197.88 – -198.01 (m), -198.03 – -198.17 (m), -198.19 – -198.33 (m). ^{13}C NMR (75 MHz, Deuterium Oxide) δ 97.33, 94.44, 49.40, 43.58. ESI MS m/z. Calc. for $[M]^+$ 145.1; Found 145.1.

Crystal growth. Corresponding carbonate (1 mmol) was dissolved in deionized water, then added 2 mmol of perchloric acid. The stirring was kept for about 10 minutes and gas bubbles were generated during the process. And then corresponding halogen salts of DABCO derivatives (2 mmol) and perchloric acid (4 mmol) were added in order. Once the acid was added, many precipitates immediately formed. Deionized Water was added continuously to dissolve the precipitates completely until the solution was clear. After slow evaporation for more than a week at room temperature, colorless and transparent block-shaped crystals were obtained and used for single-crystal X-ray diffraction. *MDAP-K*, *FMDAP-K*, *FMDAP-Rb,* and *FMDAP-Cs* were obtained according to the general method. However, during the crystal growth of *MDAP-K*, the solution needs to be wrapped to avoid light due to the sensitivity of iodized salt to light.

Methods.

Single-crystal X-ray crystallography. Variable-temperature single-crystal X-ray diffraction measurements of *MDAP-K*, *FMDAP-K*, *FMDAP-Rb*, and *FMDAP-Cs* were collected using an XtaLAB Synergy R, DW system, HyPix diffractometer equipped with a Rigaku low-temperature gas-spray cooler, with Cu Kα radiation (λ = 1.54184 Å) from a graphite monochromator. Data processing involving empirical absorption corrections was performed using the CrysAlisPro 1.171.40.82a (Rigaku Oxford Diffraction, 2020). Besides, the crystal structures were solved by direct methods and refined by the full-matrix method based on F^2 using the SHELXLTL software package. Due to the observed disorders of *MDAP-K, FMDAP-K, FMDAP-Rb* and *FMDAP-Cs* in the high-temperature phase, some restriction instructions should be adopted to handle the disordered cations. All non-hydrogen atoms were refined with anisotropy, and all H atoms were generated geometrically at the calculated positions. Drawing of asymmetric units and packing diagrams of crystals was conducted on the Diamond software. CSD deposition numbers **2402105-2402115** can be obtained free of charge from the CCDC via www.ccdc.cam.ac.uk/getstructures. The crystallographic data and structure refinement are listed in Table S1-S3, Table S5 and Table S6.

Thermal measurements. Differential scanning calorimetry (DSC) measurements of *MDAP-K*, *FMDAP-K*, *FMDAP-Rb*, and *FMDAP-Cs* were carried out on a PerkinElmer Diamond DSC instrument with a heating rate of 10 K/min under a nitrogen atmosphere.

Powder X-ray diffraction. The purity of the bulk phase was verified by powder X-ray diffraction (PXRD) measurements taken on a Rigaku D/MAX 2000 PC X-ray diffraction instrument in the 2θ range of 5-50° with a step size of 0.02°.

Dielectric measurements. For dielectric measurements, crystal samples are ground into a powder and then pressed into a thin sheet. Both sides of the sheet are covered with silver glue (the sheet does not connect) and then are secured to the electrode with copper wire. The complex dielectric constant ε ($\varepsilon = \varepsilon' - i\varepsilon''$, ε' being the real part and ε'' being the imaginary part) was measured by a TongHui TH2828A instrument.

Fluorescence spectra. Fluorescence was detected by a commercial Raman spectrometer equipped with a syncerity OE detector (Horiba, LabRAM HR Evolution) under a 325 nm He-Cd laser excitation with the reflection method. To concentrate the laser on the micrometer-sized samples, 50× microscope objectives were employed. The spectrum was separated using a diffraction grating with a groove density of 600 grooves per millimeter and recorded 3 times with an exposure duration of 3 seconds.

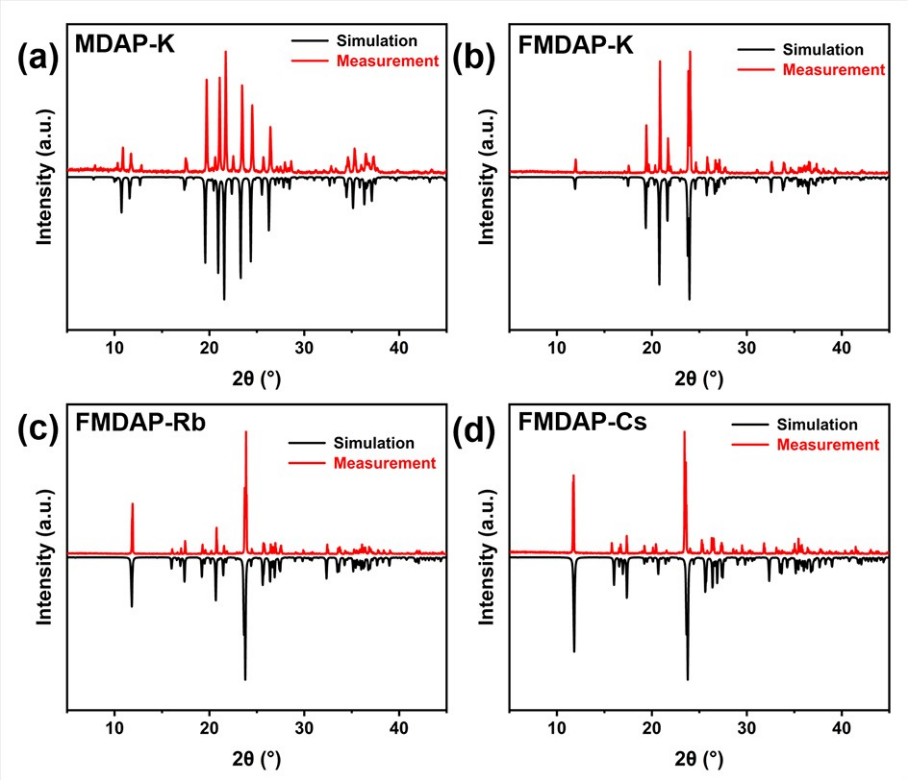

Figure S1. The PXRD patterns confirmed the phase purity of the as-synthesized sample for *MDAP-K* (a), *FMDAP-K* (b), *FMDAP-Rb* (c) and *FMDAP-Cs* (d).

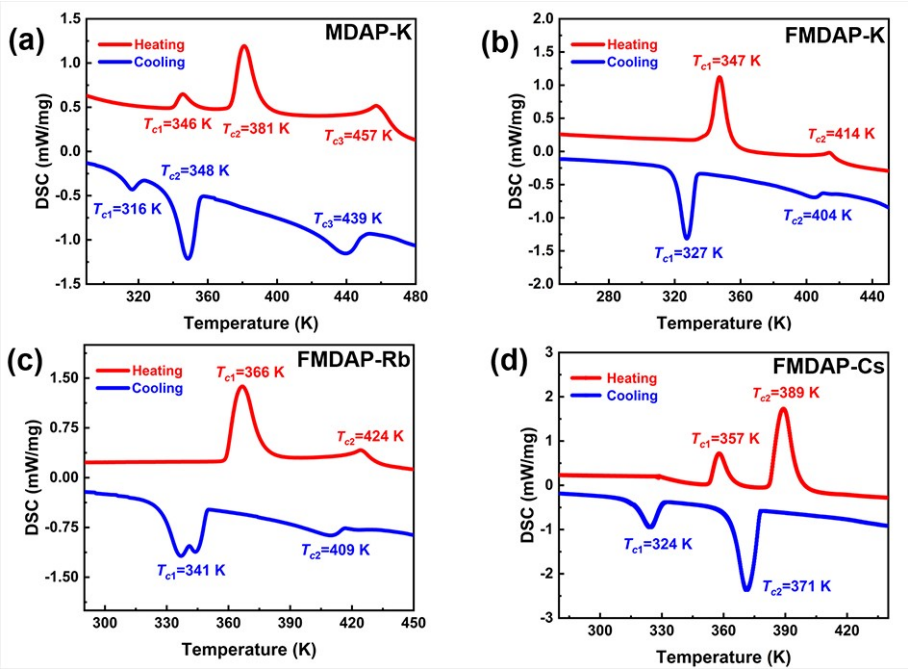

Figure S2. DSC curves of *MDAP-K* (a), *FMDAP-K* (b), *FMDAP-Rb* (c) and *FMDAP-Cs* (d).

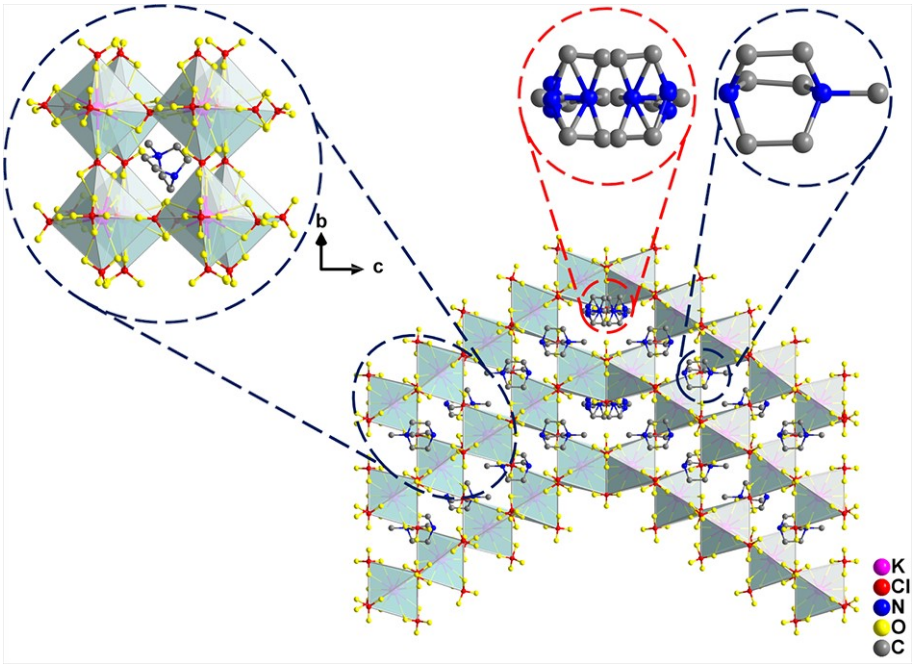

Figure S3. Crystal Structure of *MDAP-K* at 363 K

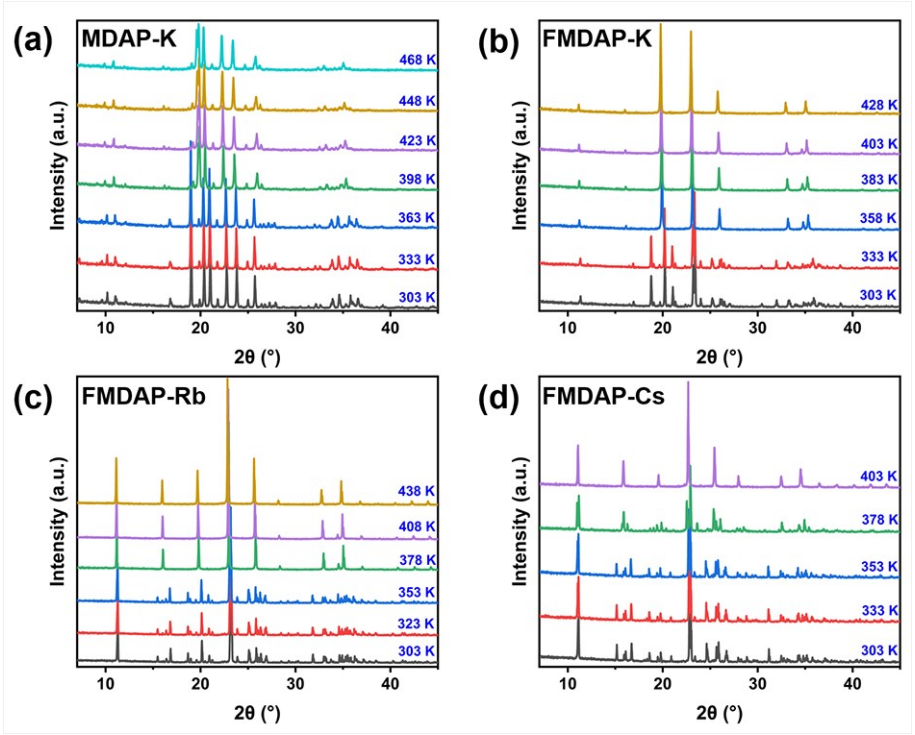

Figure S4. Measured PXRD patterns of *MDAP-K* (a), *FMDAP-K* (b), *FMDAP-Rb* (c) and *FMDAP-Cs* (d) at variable temperatures.

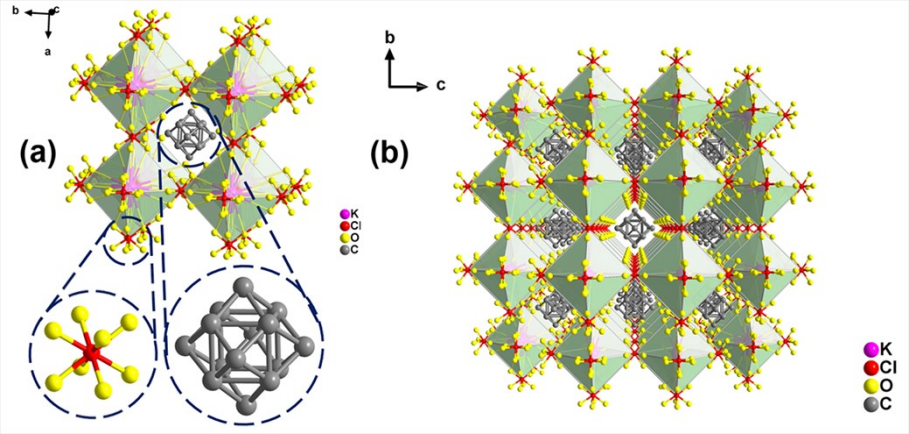

Figure S5. Molecular and stacking structures of *FMDAP-K* at 423 K.

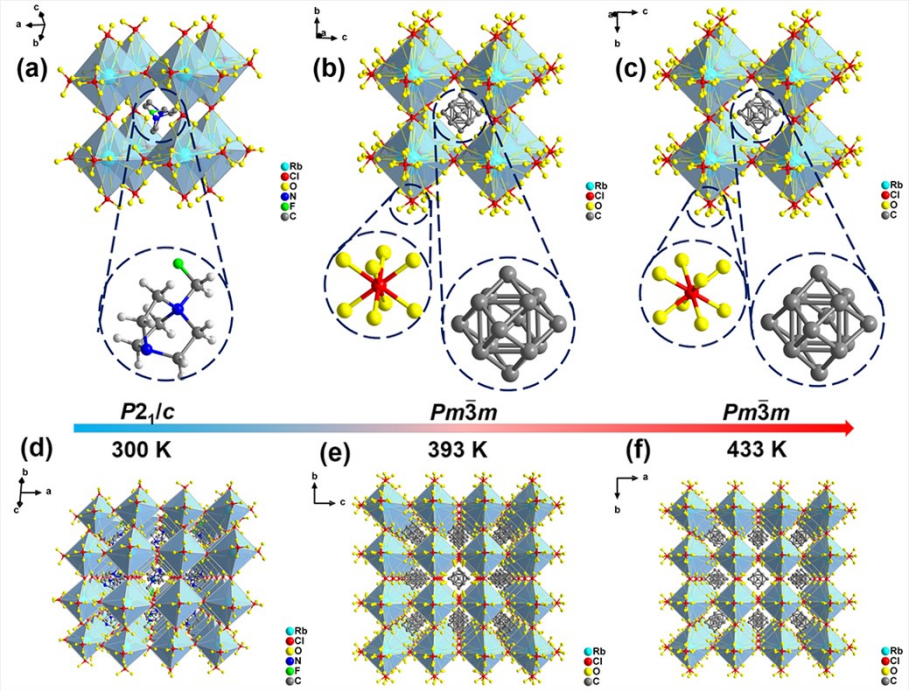

Figure S6. Molecular and stacking structures of *FMDAP-Rb* at 300 K (a and d), 393 K (b and e), and 433 K (c and f).

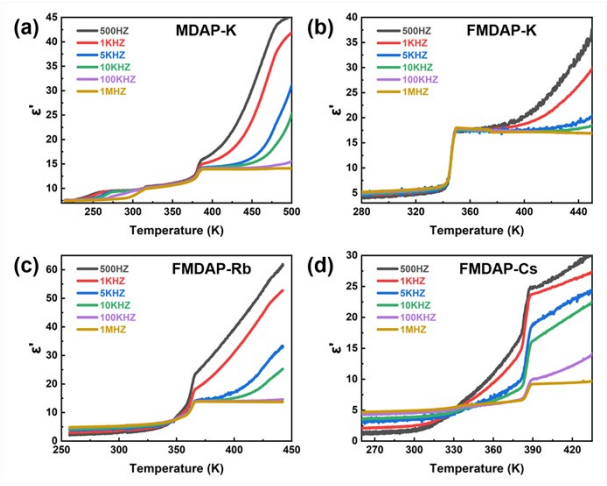

Figure S7. The ε' of *MDAP-K* (a), *FMDAP-K* (b), *FMDAP-Rb* (c) and *FMDAP-Cs* (d) measured under different frequencies in a heating run.

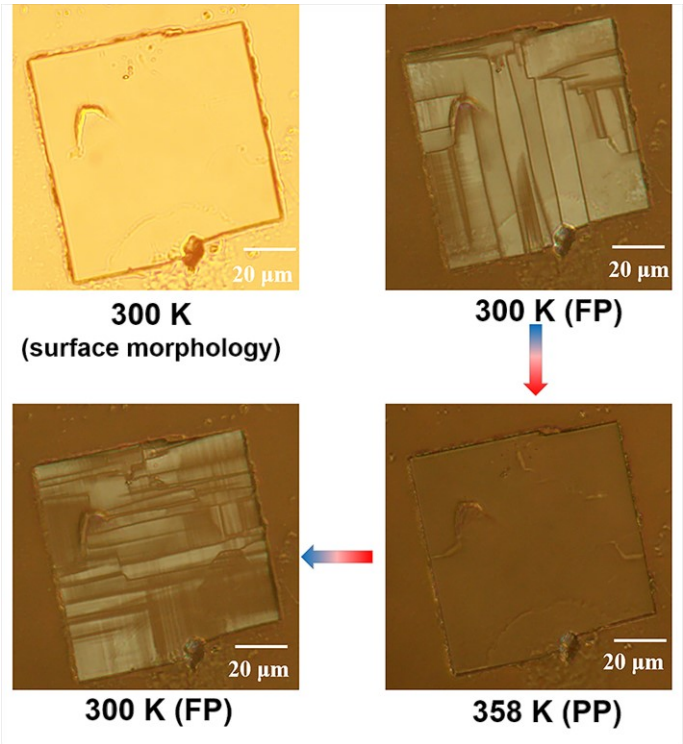

Figure S8. Evolution of ferroelastic domains repeatedly cycling between the ferroelastic phase (FP) and paraelastic phases (PP) for *FMDAP-K*.

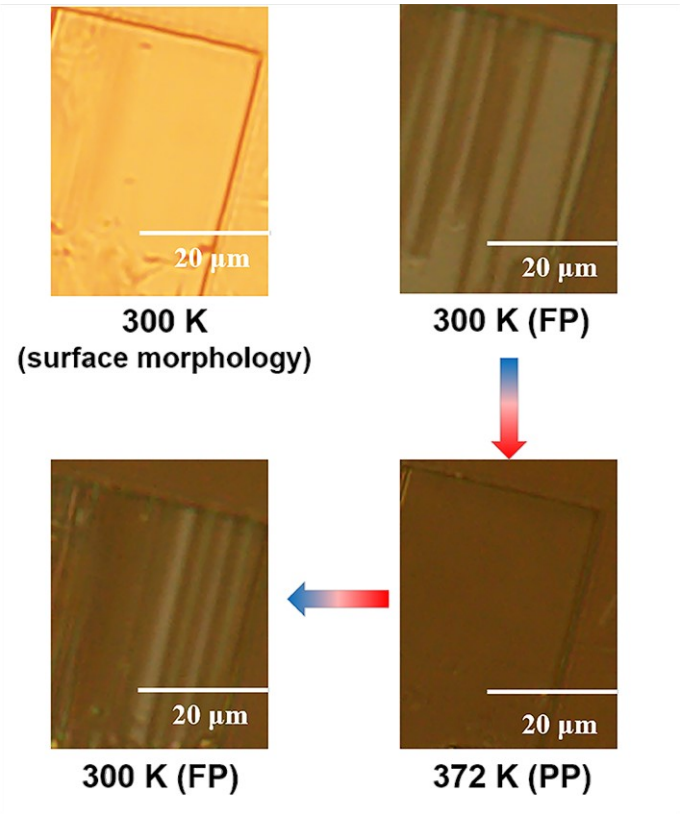

Figure S9. Evolution of ferroelastic domains repeatedly cycling between the ferroelastic phase (FP) and paraelastic phase (PP) for *FMDAP-Rb*.

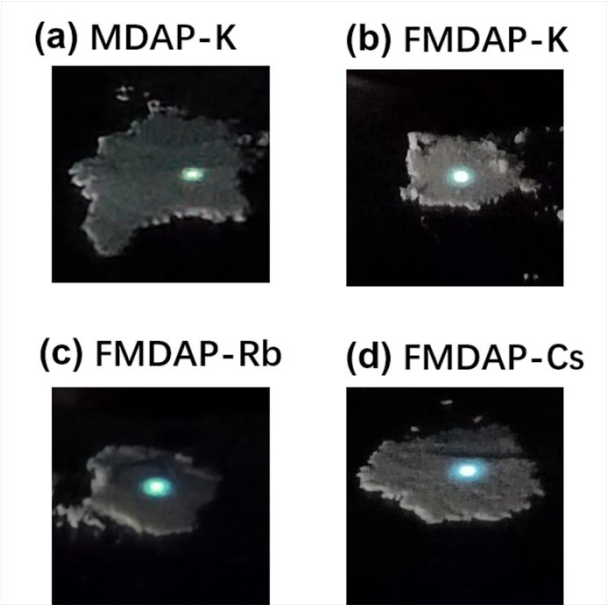

Figure S10. The optical photos of *MDAP-K* (a), *FMDAP-K* (b), *FMDAP-Rb* (c) and *FMDAP-Cs* (d) under 325 nm laser excitation.

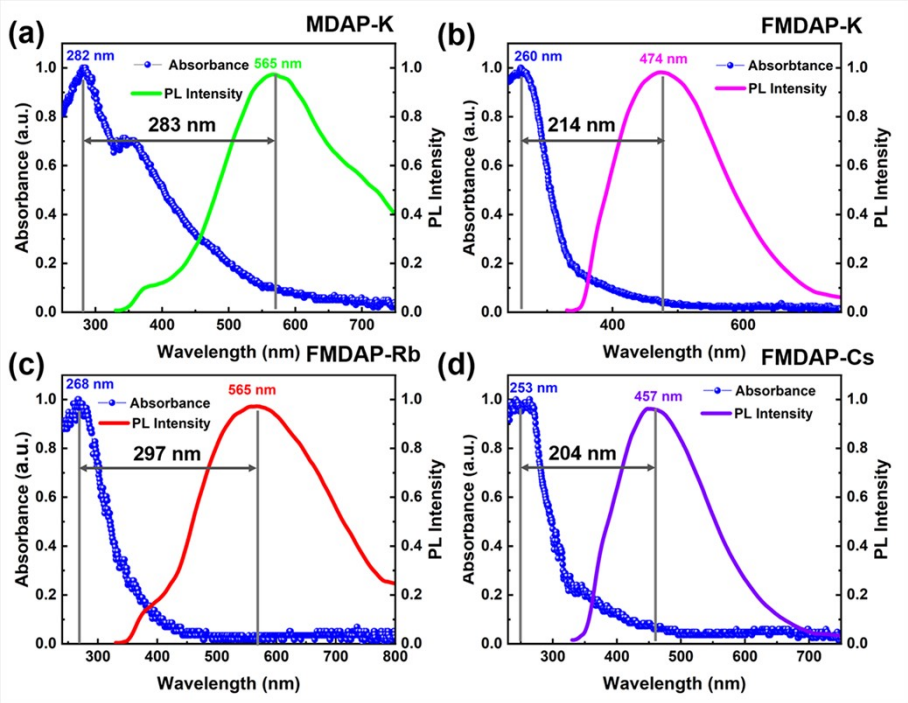

Figure S11. Normalized UV and PL spectra of *MDAP-K* (a), *FMDAP-K* (b), *FMDAP-Rb* (c) and *FMDAP-Cs* (d).

Table S1. Enthalpy and entropy changes based on the DSC measurements.

Compounds	T [K]	ΔH [J·mol^{-1}]	ΔS [J·mol^{-1}·K^{-1}]
MDAP-K	346	1862.82	5.38
	381	11700.14	30.71
	457	6003.41	13.14
FMDAP-K	347	14403.39	41.51
	414	2335.11	5.64
FMDAP-Rb	366	20692.37	56.54
	424	3709.68	8.75
FMDAP-Cs	357	8638.95	24.20
	389	28059.27	72.13

Table S2. The crystal data for *MDAP-K* at different temperatures.

Compound	***MDAP-K***	
Formula weight	450.14	449.54
Temperature/K	300 K	363 K
Crystal system	hexagonal	hexagonal
Space group	$P6_3/m$	$P6_3/m$
a/Å	10.20150(10)	10.2651(2)
b/Å	10.20150(10)	10.2651(2)
c/Å	45.3252(6)	45.4929(9)
α/°	90	90
β/°	90	90
γ/°	120	120
Volume/Å^3	4085.06(10)	4151.46(18)
Z	10	10
ρ_{calc}/g·cm^{-3}	1.830	1.798
R_{int}	0.0472	0.0369
$R_1[I>=2\sigma(I)]$	0.0493	0.0494
wR_2 $[I>=2\sigma(I)]$	0.1512	0.1577
GOF	1.046	1.061

Table S3. Hydrogen Bonds for *FMDAP-K* at 300 K

D-Hd···A	d(D-H)/Å	d(H-A)/Å	d(D-A)/Å	D-H-A/°
N1-H1···O8[1]	0.98	2.50	3.138(3)	122.6
N1-H1···O1[2]	0.98	2.01	2.900(3)	150.0
C4-H4B···O7[3]	0.97	2.60	3.273(3)	126.9
C7-H7A···O6[4]	0.97	2.77	3.470(3)	129.8
C7-H7A···O11[4]	0.97	2.61	3.375(3)	136.2
C2-H2B···O1[5]	0.97	2.71	3.360(3)	124.9
C6-H6A···O9[1]	0.97	2.74	3.354(4)	122.1
C6-H6A···O6[1]	0.97	2.40	3.140(3)	133.1
C6-H6B···O6[4]	0.97	2.68	3.448(4)	136.0
C6-H6B···O5[4]	0.97	2.52	3.470(4)	166.0
C1-H1A···O10[4]	0.97	2.32	3.251(4)	160.2
C5-H5A···O4[3]	0.97	2.61	3.427(4)	141.8
C5-H5A···O3[3]	0.97	2.37	3.293(4)	159.6
C3-H3A···O2[2]	0.97	2.60	3.202(4)	120.2
C3-H3A···O1[5]	0.97	2.85	3.493(5)	124.1

Symmetry codes: [1]+X, +Y, -1+Z; [2]2-X, 1-Y, 1-Z; [3]+X, 1/2-Y, -1/2+Z; [4]+X, 3/2-Y, -1/2+Z; [5]2-X, 1/2+Y, 3/2-Z

Table S4. The crystal data for *FMDAP-K* at different temperatures.

Compound	***FMDAP-K***		
Formula weight	483.66	433.53	433.53
Temperature/K	300 K	373 K	423 K
Crystal system	monoclinic	cubic	cubic
Space group	$P2_1/c$	$Pm\bar{3}m$	$Pm\bar{3}m$
a/Å	15.05583(19)	7.5234(6)	7.5772(10)
b/Å	10.39932(12)	7.5234(6)	7.5772(10)
c/Å	10.67058(13)	7.5234(6)	7.5772(10)
α/°	90	90	90
β/°	96.6675(11)	90	90
γ/°	90	90	90
Volume/Å^3	1659.40(3)	425.84(10)	435.04(17)
Z	4	1	1
ρ_{calc}/g·cm^{-3}	1.936	1.691	1.655
R_{int}	0.0507	0.0464	0.0352
$R_1[I>=2\sigma(I)]$	0.0416	0.1093	0.1250
wR_2 $[I>=2\sigma(I)]$	0.1249	0.2852	0.3060
GOF	1.010	1.116	0.917

Table S5. Ionic radii and the Goldschmidt tolerance factors of the corresponding perovskites.[2-4]

Compound	r_A(pm)	r_B(pm)	r_X(pm)	t
MDAP-K	268	138	238	0.952
FMDAP-K	274	138	238	0.963
FMDAP-Rb	274	152	238	0.928
FMDAP-Cs	274	167	238	0.904

Table S6. The crystal data for *FMDAP-Rb* at different temperatures.

Compound	***FMDAP-Rb***		
Formula weight	530.03	479.90	479.90
Temperature/K	300 K	393 K	433 K
Crystal system	monoclinic	cubic	cubic
Space group	$P2_1/c$	$Pm\bar{3}m$	$Pm\bar{3}m$
a/Å	15.1450(6)	7.5901(3)	7.6330(6)
b/Å	10.4572(3)	7.5901(3)	7.6330(6)
c/Å	10.7673(4)	7.5901(3)	7.6330(6)
α/°	90	90	90
β/°	96.650(3)	90	90
γ/°	90	90	90
Volume/Å^3	1693.79(11)	437.26(5)	444.72(10)
Z	4	1	1
ρ_{calc}/g·cm^{-3}	2.078	1.822	1.792
R_{int}	0.0367	0.0116	0.0617
$R_1[I>=2\sigma(I)]$	0.0419	0.0675	0.1072
wR_2 $[I>=2\sigma(I)]$	0.0946	0.1793	0.2418
GOF	1.042	0.993	1.036

Table S7. The crystal data for *FMDAP-Cs* at different temperatures.

Compound	***FMDAP-Cs***		
Formula weight	577.47	527.34	527.34
Temperature/K	300 K	363K	413K
Crystal system	monoclinic	orthorhombic	cubic
Space group	$P2_1/c$	$Cmcm$	$Pm\bar{3}m$
a/Å	15.3570(2)	10.5830(3)	7.7239(6)
b/Å	10.64331(15)	10.9576(3)	7.7239(6)
c/Å	10.84725(18)	15.4652(3)	7.7239(6)
α/°	90	90	90
β/°	97.6196(15)	90	90
γ/°	90	90	90
Volume/Å^3	1757.32(5)	1793.41(8)	460.80(11)
Z	4	4	1
ρ_{calc}/g·cm^{-3}	2.183	1.953	1.900
R_{int}	0.0653	0.1087	0.0610
$R_1[I>=2\sigma(I)]$	0.0553	0.1172	0.0647
wR_2 $[I>=2\sigma(I)]$	0.1697	0.2985	0.0316
GOF	1.140	1.278	1.163

Table S8. Summary of the luminescence properties of different compounds at room temperature.

Compound	*MDAP-K*	*FMDAP-K*	*FMDAP-Rb*	*FMDAP-Cs*
CW (nm)	565	474	565	457
FWHM(nm)	235	192	251	167
CIE (x,y)	(0.3932,0.4346)	(0.2573,0.3090)	(0.3749,0.4117)	(0.2390,0.2772)
CCT [K]	4063	11276	4360	19390
CRI	83	82	88	84

Note: Central wavelength (CW), full width at half-maximum (FWHM), Commission Internationale de l'Eclairage chromaticity coordinates (ClE), correlated color temperature (CCT), color rendering indexes (CRI).

References:

1. J. Y. Kazock, M. Taggougui, B. Carré, P. Willmann and D. Lemordant, Simple and efficient synthesis of *N*-quaternary salts of quinuclidinium derivatives, *Synthesis*, 2007, **2007**, 3776-3778.
2. S. D. Gale, H. J. Lloyd, L. Male, M. R. Warren, L. K. Saunders, P. A. Anderson and H. H. M. Yeung, Materials discovery and design limits in MDABCO perovskites, *CrystEngComm*, 2022, **24**, 7272-7276.
3. Y. L. Sun, X. B. Han and W. Zhang, Structural phase transitions and dielectric switchings in a series of organic-inorganic hybrid perovskites ABX_3 ($X = ClO_4^-$ or BF_4^-), *Chem. Eur. J*, 2017, **23**, 11126-11132.
4. M. J. Sun, C. Zheng, Y. Gao, A. Johnston, A. M. Najarian, P. X. Wang, O. Voznyy, S. Hoogland and E. H. Sargent, Linear Electro-Optic Modulation in Highly Polarizable Organic Perovskites, *Adv. Mater.*, 2021, **33**, 2006368.